

Observation of Anomalous Plasmon Linewidth in the Icosahedral Al-Mn Quasicrystals

C. H. Chen, D. C. Joy, H. S. Chen, and J. J. Hauser

AT&T Bell Laboratories, Murray Hill, New Jersey 07974

(Received 21 April 1986)

The linewidth of bulk plasmons in a rapid-quench Al_6Mn quasicrystal is found to increase by $\sim 40\%$ as compared with that observed in a thermally annealed crystalline Al_6Mn sample. A narrower plasmon linewidth is also observed in a sputtered amorphous Al_6Mn thin-film sample. We believe that the unusual plasmon line broadening in Al_6Mn quasicrystals is a result of increased interband transitions due to the icosahedral symmetry of the quasicrystal, and not a consequence of lattice disorder.

PACS numbers: 71.45.Gm, 71.25.Mg, 79.20.Kz

Since the exciting discovery of the icosahedral symmetry in rapidly quenched Al_6Mn alloys ($i\text{-Al}_6\text{Mn}$) by Shechtman *et al.*,¹ systems with icosahedral symmetry have captured the attention of physicists and material scientists around the world. The appearance of sharp diffraction spots can now be understood by a new class of ordered structures (quasicrystals) with quasiperiodic rather than periodic translational order.² Almost all papers published so far in this rapidly growing field have dealt with the lattice structure in one form or another in an attempt to unravel the ultimate mystery, i.e., exactly where the atoms are located in the lattice. On the other hand, experimental probes of the electronic properties of $i\text{-Al}_6\text{Mn}$ have so far revealed nothing unusual. In this Letter we report the first experimental observation of the excitation spectra of the electron gas in Al-Mn quasicrystals by high-energy transmission electron-energy-loss spectroscopy (EELS), and we show a significant ($\sim 40\%$) plasmon line broadening in the icosahedral phase as compared with that observed in its crystalline counterpart ($c\text{-Al}_6\text{Mn}$). We argue that this is due to the change of electronic structure in the $i\text{-Al}_6\text{Mn}$ phase.

Samples of $i\text{-Al}_6\text{Mn}$ quasicrystals were made by induction melting of high-purity Al and Mn in boron nitride crucibles under argon atmosphere. Ribbons of ~ 1 mm in width and $30 \mu\text{m}$ in thickness were obtained by melt spinning in an argon atmosphere on a copper wheel. The thin-film samples for EELS were prepared by chemical thinning. Amorphous Al_6Mn samples ($\sim 500 \text{ \AA}$ in thickness) were prepared on rock-salt substrate by sputtering. EELS was carried out in a VG H5 100-kV scanning transmission electron microscope equipped with a Gatan 607 electron spectrometer. A $5\text{--}10 \text{ \AA}$ electron probe was used to probe the electronic and chemical inhomogeneities in real space. An energy resolution of $\sim 0.7 \text{ eV}$ was routinely obtained with a collection angle of $\sim 15 \text{ mrad}$. The energy-loss spectra were obtained by electrostatic scanning of the drift tube of the magnetic spectrometer and, therefore, precise peak positions could be deter-

mined.

The application of microprobe analysis is most suitable for studies of Al-Mn quasicrystals which are formed through complex nucleation and growth

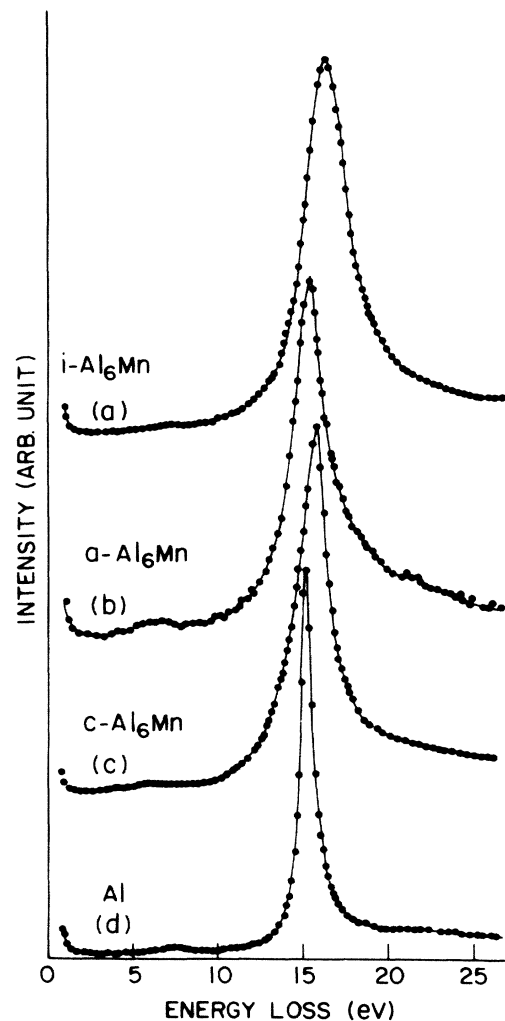


FIG. 1. Plasmon spectra for Al, $c\text{-Al}_6\text{Mn}$, $a\text{-Al}_6\text{Mn}$, and $i\text{-Al}_6\text{Mn}$.

processes. The materials have long been thought to be quite inhomogeneous. It is well known that rapidly quenched $i\text{-Al}_6\text{Mn}$ quasicrystals are characterized by large domains ($\sim 1 \mu\text{m}$ in size) with elongated branches stemming from a central nodule within the domain.¹ An energy-loss spectrum obtained by placing the electron probe within a branch of an icosahedral domain is shown in Fig. 1(a). We see that the spectrum is dominated by a bulk-plasmon excitation peak at ~ 16 eV with a full width at half maximum $\Delta E_{1/2} \approx 3.1$ eV. A weak peak at ~ 6.5 eV is also seen, which we identify as due to surface-plasmon excitations. By placing the electron microprobe at boundaries between the domains or boundaries which separate branches within a domain, a totally new spectrum is observed as shown in Fig. 1(d). Figure 1(d) reveals a much narrower bulk-plasmon peak ($\Delta E_{1/2} \approx 1.2$ eV) at 15.3 eV which is characteristic of the presence of pure Al. The Al precipitation during the growth of $i\text{-Al}_6\text{Mn}$ quasicrystals is best demonstrated by the plasmon imaging technique in which the electron spectrometer is preset at a particular energy loss while the electron microprobe is scanning across the area of interest on the sample. Figure 2 shows a scanning transmission electron microscope dark-field image of an icosahedral domain together with plasmon images obtained from pure Al peak at 15.3 eV [Fig. 1(d)] and $i\text{-Al}_6\text{Mn}$ peak at 16.2 eV [Fig. 1(a)]. A reversal of contrast is seen between Figs. 2(b) and 2(c) as expected. Figure 2(b) clearly shows that the boundaries, either between the domains, or between the branches within a domain, are filled with pure Al. The plasmon energy within an $i\text{-Al}_6\text{Mn}$ branch is found to vary from 15.7 to ~ 16.5 eV by placing the 5–10 Å probe on various spots. Nevertheless, the plasmon linewidth remains unchanged. This variation of plasmon energy is clearly due to change of the Mn concentration, a finding confirmed by simultaneous x-ray microanalysis. We find that spatial homogeneity is ≤ 200 Å. Considering the finite thickness (~ 500 Å) of the sample and the preferential forward scattering of the high-energy electrons, we estimate the spatial resolution of our microprobe plasmon measurement to be ≤ 20 Å. Assuming a rigid-band free-electron gas model and starting with a plasmon energy of 15.3 eV for Al, we can estimate the plasmon energy of Al_6Mn alloy to be 16 eV, which is in good agreement with the values that we observed. The variation of the observed plasmon energy would then correspond to a $\sim 10\%$ fluctuation in Mn concentration over a 200-Å scale.

Thermal annealing at 700 K for 20 h in vacuum transforms $i\text{-Al}_6\text{Mn}$ into a crystalline phase with orthorhombic symmetry ($c\text{-Al}_6\text{Mn}$). Plasmon spectra obtained from the $c\text{-Al}_6\text{Mn}$ grains exhibit a much narrower ($\Delta E_{1/2} \approx 2.2$ eV) peak at similar energies



FIG. 2. (a) Scanning transmission electron microscope dark-field image of a domain in $i\text{-Al}_6\text{Mn}$; (b) energy-filtered image of the same area with spectrometer pass energy set for the 15.3-eV (Al) loss peak; (c) image of the same area with spectrometer pass energy set for the 16.2-eV ($i\text{-Al}_6\text{Mn}$) loss peak. Note the reversal of contrast in (b) and (c). The fine periodic lines that appear in (b) and (c) are due to instrumental artifacts.

(15.7–16.0 eV), as also shown in Fig. 1(c). We note that the plasmon linewidth increases significantly by 40% from the $c\text{-Al}_6\text{Mn}$ phase to the $i\text{-Al}_6\text{Mn}$. It is well known that plasmons in metals decay primarily via interband transitions.^{3–5} The effects of lattice order on the plasmon linewidth have been shown to be small in both semiconductors and metals as summarized in Table I. In particular, amorphous Si and Ge have

TABLE I: Experimental plasmon linewidths $\Delta E_{1/2}$ (in electronvolts) for Si, Ge, Sn, Hg, Ga, and Al_6Mn . c denotes crystalline; a denotes amorphous; liq. denotes liquid; i denotes icosahedral.

	c	a	liq.	i
Si	3.7	3.9		
Ge	3.4	3.6		
Sn	1.6		1.6	
Hg	1.5		1.0	
Ga	1.4		1.15	
Al_6Mn	2.2	2.4		3.1

linewidths $\Delta E_{1/2} \approx 3.9$ eV and 3.6 eV, only $\sim 5\%$ higher than their crystalline counterparts with $\Delta E_{1/2} \approx 3.7$ and 3.4 eV, respectively.⁶ Plasmons in Sn metals have the same linewidth ($\Delta E_{1/2} \approx 1.6$ eV), regardless of whether Sn metal is in the form of crystal or liquid.⁷ Furthermore, liquid Hg and Ga even show a narrower plasmon linewidth ($\Delta E_{1/2} \approx 1.0$ eV) than their crystalline counterparts ($\Delta E_{1/2} \approx 1.5$ eV).^{7,8} All these existing experimental data clearly suggest that lattice disorder is not of any primary significance in the plasmon linewidth. To further prove our point, we have, in fact, obtained bulk-plasmon spectra from amorphous Al_6Mn ($a\text{-Al}_6\text{Mn}$) as shown in Fig. 1(b). The plasmon linewidth of $a\text{-Al}_6\text{Mn}$, $\Delta E_{1/2} \approx 2.4$ eV, is indeed smaller than that of $i\text{-Al}_6\text{Mn}$. Because of the presence of carbon contamination buildup in the sputtered $a\text{-Al}_6\text{Mn}$ film under the electron-beam irradiation, the broad plasmon peak of the carbon contamination at ~ 23 eV could give some contribution to the observed plasmon linewidth in $a\text{-Al}_6\text{Mn}$. The actual linewidth should be slightly smaller than the observed value of 2.4 eV. This clearly shows that the lattice disorder has very little effect on the plasmon linewidth in binary alloys.

We believe that the much broader plasmon peak observed in $i\text{-Al}_6\text{Mn}$ is due to the change of electronic band structure which provides many more decay channels for plasmons via interband transitions. As a result of the presence of incommensurate lattice spacing defined by the golden mean, $(1 + \sqrt{5})/2$, it is expected that changes of energy bands should occur throughout the reciprocal lattice and allow many new channels for interband transitions. Most recent numerical calculations of the electron and phonon spectra for quasicrystals⁹⁻¹³ have, in fact, confirmed the existence of many gaps and Van Hove singularities near the band edge. The self-similarity of the lattice has also been shown to produce hierarchical bands and an infinite density of gaps in the excitation spectra. Our observation of plasmon linewidth, therefore, provides the first experimental evidence for the dramatic change of electronic structure in $i\text{-Al}_6\text{Mn}$.

In a high-energy transmission EELS measurement, the scattering cross section is proportional to the so-called energy-loss function, $\text{Im}[-1/\epsilon(\omega)]$, where $\epsilon(\omega)$ is the frequency-dependent dielectric function. The wave-vector dependence of ϵ is not considered in our case since it was integrated automatically in our measurement by the angular spread of the electron probe. One can show that the plasmon linewidth $\Delta E_{1/2}$ is related to the dielectric function as

$$\Delta E_{1/2} = 2\epsilon_2(\omega_p)(d\epsilon_1/d\omega)_{\omega_p}^{-1}, \quad (1)$$

where ϵ_1 and ϵ_2 are the real and imaginary parts of the dielectric function and ω_p is the plasmon frequency. From Eq. (1) it is clear that a significant increase of $\Delta E_{1/2}$ does not necessarily come from a big increase of $\epsilon_2(\omega_p)$. Small changes of the shape of $\epsilon(\omega)$, which become observable through the derivative $(d\epsilon_1/d\omega)_{\omega_p}$, can also play a significant role in the plasmon linewidth. In the energy-loss spectra of $i\text{-Al}_6\text{Mn}$, we did not observe any distinct peak above 1.5 eV which can be attributed to interband transitions. It is well known that poorly defined weak interband transitions with their oscillator strength spreading out in wide energy ranges are not readily visible in experiments. However, their effects can add up and become visible in $\Delta E_{1/2}$ according to Eq. (1). This can be easily understood with a simple Drude dielectric model including interband transitions, which can be written as

$$\epsilon(\omega) = 1 - \frac{\omega_p^2}{\omega(\omega + i\gamma)} - \frac{4\pi e^2}{m} \sum_i \frac{f_i}{(\omega^2 - \omega_i^2) + i\omega\tau_i}, \quad (2)$$

where γ and τ_i are the damping factors for plasmons and interband transitions, respectively. ω_i and f_i are the frequency and oscillator strength of the interband transitions. From Eq. (2) it is clear that the presence of interband transitions will tend to increase ϵ_2 near the plasmon frequency ω_p , and, therefore, give rise to further broadening of plasmons. The effects of interband transitions on plasmons have been well treated in the literature.^{3,14} Given the high density of energy gaps in the quasicrystals, it is expected that interband transitions should play a significant role in the plasmon linewidth. We believe that an increase of $\epsilon_2(\omega)$ and a decrease of the slope of $\epsilon_1(\omega)$ near ω_p are responsible for the increase of plasmon linewidth in $i\text{-Al}_6\text{Mn}$ quasicrystals. We note that, in general, the plasmon energy is shifted by interband transitions. The fact that our observed plasmon energy falls close to the calculated value of 16 eV suggests that the interband transitions above the plasmon largely cancel the shift due to interband transitions below the plasmon.

In conclusion, we have shown convincingly that the plasmon line broadening in $i\text{-Al}_6\text{Mn}$ is due to increased channels of interband transitions as a result of

icosahedral symmetry and not due to increased disorder of the lattice. Small-electron-probe (5–10 Å) analysis of electronic excitations reveals that rapidly quenched δ -Al₆Mn quasicrystals are spatially very inhomogeneous.

¹D. Shechtman, I. Blech, D. Gratias, and J. W. Cahn, *Phys. Rev. Lett.* **53**, 1951 (1984).

²D. Levine and P. J. Steinhardt, *Phys. Rev. Lett.* **53**, 2477 (1984).

³K. Sturm, *Adv. Phys.* **31**, 1 (1982), and *Z. Phys. B* **28**, 1 (1977).

⁴M. Hasegawa and M. Watabe, *J. Phys. Soc. Jpn.* **27**, 1393

(1969).

⁵M. Hasegawa, *J. Phys. Soc. Jpn.* **31**, 649 (1971).

⁶T. Aiyama and K. Yada, *J. Phys. Soc. Jpn.* **36**, 1554 (1974).

⁷K. Zeppenfeld, *Z. Phys.* **223**, 32 (1969).

⁸H. Boersch, J. Geiger, H. Hellwig, and H. Michel, *Z. Phys.* **169**, 252 (1962).

⁹T. C. Choy, *Phys. Rev. Lett.* **55**, 2915 (1985).

¹⁰T. Odagaki and D. Nguyen, *Phys. Rev. B* **33**, 2184 (1986).

¹¹J. P. Lu, T. Odagaki, and J. L. Birman, *Phys. Rev. B* **33**, 4809 (1986).

¹²F. Nori and J. P. Rodriguez, to be published.

¹³M. A. Marcus, to be published.

¹⁴For example, see H. Raether, *Springer Tracts in Modern Physics*, Vol. 38 (Springer-Verlag, New York, 1965), p. 85.

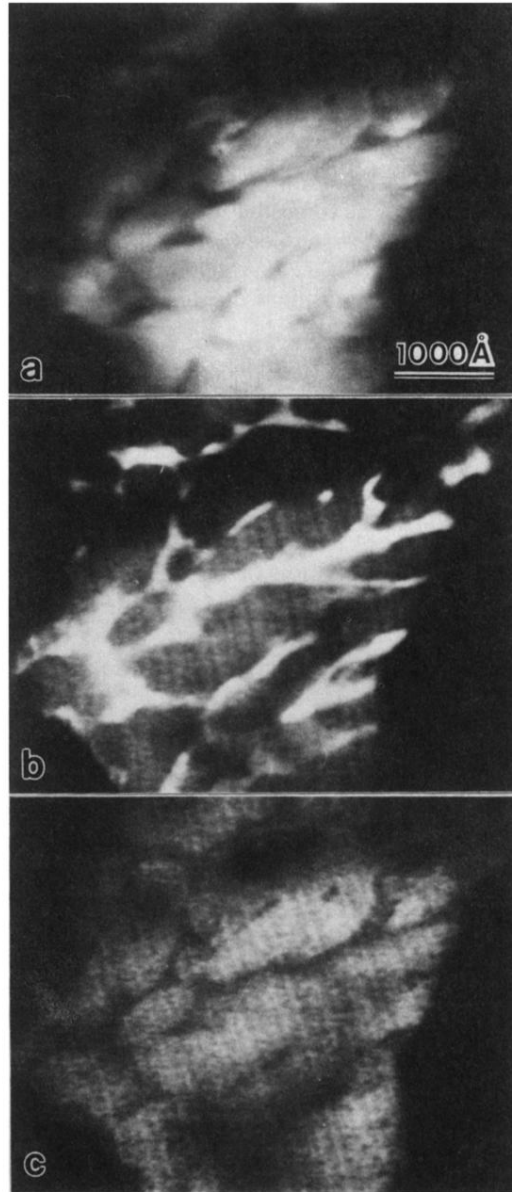


FIG. 2. (a) Scanning transmission electron microscope dark-field image of a domain in $i\text{-Al}_6\text{Mn}$; (b) energy-filtered image of the same area with spectrometer pass energy set for the 15.3-eV (Al) loss peak; (c) image of the same area with spectrometer pass energy set for the 16.2-eV ($i\text{-Al}_6\text{Mn}$) loss peak. Note the reversal of contrast in (b) and (c). The fine periodic lines that appear in (b) and (c) are due to instrumental artifacts.